

Cascaded FSO-VLC Communication System

Akash Gupta, *Student Member, IEEE*, Nikhil Sharma, *Member, IEEE*, Parul Garg, *Senior Member, IEEE*, and Mohamed-Slim Alouini, *Fellow, IEEE*

Abstract—The proposed cascaded free space optics (FSO)-visible light communication (VLC) system consists of multiple VLC access points which caters the end users connected via a decode and forward (DF) relay to the FSO backhaul link. The FSO link is assumed to be affected by path-loss, pointing error and atmospheric turbulence while the end-to-end signal-to-noise ratio (SNR) of VLC downlinks are statistically characterized considering the randomness of users position. In this study, the novel closed form expressions of the statistics like probability density function (PDF) and cumulative distribution function (CDF) of the equivalent SNR are derived. Capitalizing on these, the closed form expressions for various performance metrics such as outage probability and error probability are provided. The simulation results are provided to verify the functional curves of mathematical analysis.

Index Terms—FSO, VLC, DF relay, BER.

I. INTRODUCTION

Optical wireless communication (OWC) systems have garnered attention from academia and industries owing to its large unlicensed spectrum. The OWC makes use of complete optical spectrum from infrared to ultraviolet, including the visible light range. Visible light communication (VLC) has emerged as an attractive alternative for indoor radio frequency (RF) communication and can fulfill the ever increasing demands for heavy data services. Besides offering a huge and unlicensed bandwidth to cope with crowded radio spectrum, the VLC technology possesses various other merits such as ease of availability, radiation free and no electromagnetic interference. On the other hand, free space optical (FSO) communication system, which is a line-of-sight (LOS) technology, has attracted significant attention as high bandwidth last mile transmission technique. FSO is a reasonable alternative to optical fibers as it requires less initial deployment [1] and can be installed at locations where deployment wired connection is challenging.

The indoor VLC system must be connected to the base station to realize the communication purpose. The most economical solution for connecting indoor VLC system to outside base station is by using power cables. In this context, various studies [2], [3] have been proposed involving the integration of VLC with power line communication (PLC) as the backbone network. However, the PLC channel suffer

from several impairments: deep notches, high attenuation and colored background noise that limits the data rate. To provide better data rate and improve the system performance, the VLC system should be complimented by high bandwidth FSO link that enables high data rate in-door multimedia services. In [4], authors have experimentally demonstrated a direct FSO/VLC heterogenous interconnection with data aggregation and distribution. However, the FSO/VLC system has not been statistically analysed and its performance under various parametric variations has not been studied.

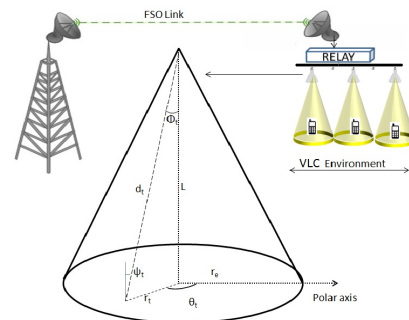


Figure 1: System model of the mixed FSO/VLC communication system.

Thus, motivated by the above facts the major contributions of this paper are listed as follows. 1) A deeply integrated FSO and VLC system model is proposed for in-door multimedia broadcasting. 2) The novel closed-form expressions of the statistics (probability density function (PDF) and cumulative distribution function (CDF)) of the end-to-end signal-to-noise ratios (SNRs) are proposed in this study. 3) Various performance metrics like outage probability and average error rate are derived by using the channel statistics. 4) We analyze the proposed system and obtain performance results for different atmospheric conditions, distinct room sizes, and varying number of LEDs. 5) Simulations are performed to verify the theoretical results.

II. SYSTEM MODEL

We consider a cascaded FSO-VLC communication system which realizes the downlink transmission scenarios and covers a large indoor area as shown in Fig. 1. The system model consists of an FSO link that acts as a back-haul link for providing access to the backbone network. On the other hand, there are multiple VLC access points located on the ceiling and T mobile users are uniformly distributed over the coverage area. The indoor VLC system is connected to the FSO link via a decode and forward (DF) relay. The relay decodes the signal from the FSO link and retransmits it on the visible light frequency. At the user terminal the photo-detectors converts

Akash Gupta and Parul Garg, are with the Division of Electronics and Communication Engineering, Netaji Subhas Institute of Technology, Sector 3 Dwarka, New Delhi 110078, India (E-mail: akashgeminii@gmail.com, parul_sainii@yahoo.co.in). Nikhil Sharma is with the Division of Electronics and Communication Engineering, LNMIIIT, Jaipur, India. (E-mail: nikhilsharma.nit90@gmail.com). M.S. Alouini is with the Computer, Electrical, and Mathematical Sciences, and Engineering (CEMSE) Division, King Abdullah University of Science and Technology (KAUST), Thuwal, Makkah Province, Saudi Arabia (E-mail: slim.alouini@kaust.edu.sa).

the optical signal into electrical signal through direct detection technique.

Although VLC channels incorporate both LOS and diffuse components, it is observed in [5], that the energy of the reflected signal is much lower than the energy of the LOS. Thus, it is assumed that each user is served by a single VLC access point (AP) which has the strongest channel gain for that user. All the VLC AP utilize the same bandwidth thus there will be intercell interference (ICI). In this study we have treated ICI as a Gaussian noise [6].

The LED lamp as shown in Fig. 1 is placed at height L from the t -th end user located with angle θ_t and radius r_t on the polar coordinate plane. The maximum radius covered by an LED cell is r_e . It is observed in [5], that the LED follows a Lambertian radiation pattern with order $m = -1/\log_2(\cos(\phi_{1/2}))$, where $\phi_{1/2}$ represents the semi-angle of LED. Ψ_{FOV} denotes the field of view (FOV) of the receiver. The angle of incidence and angle of irradiance are denoted by ψ_t and ϕ_t , respectively. It is observed from [5], that the DC channel gain of the LOS link between LED and t -th user is given as

$$h_t = \frac{A(m+1)R_p}{2\pi d_t^2} \cos^m(\phi)U(\psi_t)g(\psi_t) \cos(\psi_t) \quad , \quad (1)$$

where A denotes the detector area, R_p represents the responsivity of photo-detector, d_t is the Euclidean distance between LED and t -th user, $U(\Psi_t)$ and $g(\Psi_t)$ represent the gain of optical filter and optical concentrator [5], respectively.

III. CHANNEL MODEL

In the proposed cascaded FSO-VLC downlink communication system, the terrestrial FSO link is assumed to be Gamma-Gamma distributed taking into account the combined effect of path loss (I_l), atmospheric turbulence (I_a) and pointing error (I_p), while the VLC links are subjected to distribution based on the uniformly distributed location of end users.

A. Free Space Optical (FSO) Fading Channel Model

The terrestrial FSO link is assumed to follow a unified Gamma-Gamma distribution with pointing error impairments. The PDF of the instantaneous SNR Γ_{FSO} is written as in [7], as

$$f_{\Gamma_{FSO}}(\gamma) = \frac{\xi^2}{q\gamma\Gamma(\alpha)\Gamma(\beta)} \mathcal{G}_{1,3}^{3,0} \left[d\alpha\beta \left(\frac{\gamma}{k_q} \right)^{1/q} \middle| \begin{matrix} \xi^2+1 \\ \xi^2, \alpha, \beta \end{matrix} \right] \quad , \quad (2)$$

where $\mathcal{G}(\cdot)$ is the Meijer-G function, q accounts for detection technique (i.e. $q = 1$ represents heterodyne detection and $q = 2$ represents direct detection), $d = \xi^2/(\xi^2 + 1)$, $\xi = w_e/2\sigma_s$, w_e is the equivalent beam-width, σ_s denotes the standard deviation of pointing error distribution. Further k_q denotes the average electrical SNR. More specifically, for k_q , when $q = 1$, $k_q = \mathbb{E}(\gamma)$ and when $q = 2$, $k_q = \bar{\gamma} \alpha \beta \xi^2 (\xi^2 + 1) / [(\alpha + 1)(\beta + 1)(\xi^2 + 1)^2]$ where the average SNR of the FSO link $\bar{\gamma} = \mathbb{E}[\gamma]$ with \mathbb{E} representing expectation operator. The two fading parameters α and β , which determine the atmospheric conditions are given as in [8].

B. Visible Light Communication (VLC) Fading Channel Model

The channel model for the VLC link is based on the uniform distribution of the location of end users [9]. From Fig. 1 we can find the angle of irradiance (ϕ_t), angle of incidence (ψ_t) and the Euclidian distance (d_t) for the t -th user in terms of height (L) and the radical distance (r_t) as $\cos(\psi) = \cos(\phi) = \frac{L}{d_t}$ and $d_t = (r_t^2 + L^2)^{1/2}$. Substituting these in (1), we get the DC gain for the LOS component as

$$h_t = \frac{\Xi(m+1)L^{m+1}}{(r_t^2 + L^2)^{\frac{m+3}{2}}} \quad , \quad (3)$$

where $\Xi = \frac{1}{2\pi} AR_p U(\psi_t)g(\psi_t)$ is a constant for a considered system. It is clearly seen from (3), that the DC channel gain (h_t) is inversely proportional to the radical distance of the user (r_t). Further in order to obtain a statistical model of channel gain (h_t), the user position is considered to be random and assuming r_t to be following a uniform distribution with PDF given as $f_{r_t}(r) = \frac{2r}{r_e^2}$. The PDF of channel gain can be derived using the change of variable method [10] and is given as,

$$f_{h_t}(h) = \frac{2}{r_e^2(m+3)} (\Xi(m+1)L^{m+1})^{\frac{2}{m+3}} h^{-\frac{2}{m+3}-1} \quad (4)$$

Consequently, the PDF of the instantaneous SNR $\gamma_{VLC} = \bar{\gamma}_{VLC} h_t^2$, using (4) is given as

$$f_{\Gamma_{VLC}}(\gamma) = \frac{\bar{\gamma}_{VLC}^{\frac{1}{m+3}}}{r_e^2(m+3)} (\Xi(m+1)L^{m+1})^{\frac{2}{m+3}} \gamma^{-\frac{m+4}{m+3}} \quad (5)$$

for $\gamma \in [\lambda_{min}, \lambda_{max}]$, where $\lambda_{min} = \frac{\bar{\gamma}_{VLC}(\Xi(m+1)L^{m+1})^2}{(r_e^2 + L^2)^{m+3}}$, $\lambda_{max} = \frac{\bar{\gamma}_{VLC}(\Xi(m+1)L^{m+1})^2}{L^{2(m+3)}}$ and $\bar{\gamma}_{VLC} = \frac{\rho^2 P_{opt}^2}{N_o B}$. Here ρ is electrical to optical conversion efficiency, P_{opt} is transmitted optical power, N_o being noise spectral density and B is the baseband modulation bandwidth. On integrating (5) we obtain the CDF as

$$F_{\Gamma_{VLC}}(\gamma) = \frac{-1}{r_e^2} (\Xi(m+1)L^{m+1})^{\frac{2}{m+3}} \left(\frac{\gamma}{\bar{\gamma}_{VLC}} \right)^{\frac{-1}{m+3}} + \left(1 + \frac{L^2}{r_e^2} \right) \quad (6)$$

IV. STATISTICS OF THE SNR OF EQUIVALENT END-TO-END LINK

In this section, the novel analytical expressions of CDF and PDF of equivalent end to end SNR of DF relay based FSO/VLC mixed cascaded system are derived.

A. Cumulative Distribution Function

The CDF of equivalent end to end SNR (Γ_{eq}) for the proposed cascaded FSO-VLC system is given as in [11] as

$$\mathcal{F}_{\Gamma_{eq}}(\gamma) = \Pr[\min(\Gamma_{FSO}, \Gamma_{VLC}^{max}) < \gamma] \quad , \quad (7)$$

where Γ_{VLC}^{max} represents the SNR of the best link amongst the multiple VLC links. Assuming the FSO and VLC links to be independent we can rewrite (7) as

$$\mathcal{F}_{\Gamma_{eq}}(\gamma) = \Pr(\Gamma_{FSO} < \gamma) + \Pr(\Gamma_{VLC}^{max} < \gamma) - \Pr(\Gamma_{FSO} < \gamma)\Pr(\Gamma_{VLC}^{max} < \gamma) \quad , \quad (8)$$

using (2) $\Pr(\Gamma_{FSO} < \gamma)$ can be evaluated as

$$\Pr(\Gamma_{FSO} < \gamma) = \mathcal{F}_{\Gamma_{FSO}}(\gamma) = \frac{\xi^2 2^{\alpha+\beta-2}}{\Gamma(\alpha)(2\pi)} \gamma^{\alpha+\beta-1} \times \mathcal{G}_{3,7}^{6,1} \left(\left. \frac{(d\alpha\beta)^2 \gamma}{16k_2 \bar{\gamma}_{FSO}} \right|_{\tau}^{\omega} \right) \quad (9)$$

where $\omega = 1, \frac{\xi^2+1}{2}, \frac{\xi^2+2}{2}$ and $\tau = \frac{\xi^2}{2}, \frac{\xi^2+1}{2}, \frac{\alpha}{2}, \frac{\alpha+1}{2}, \frac{\beta}{2}, \frac{\beta+1}{2}, 0$

The user terminal is connected with the VLC access point that offers the maximum SNR. Thus, the CDF of the SNR of the best possible VLC link can be given as

$$\mathcal{F}_{\Gamma_{VLC}^{max}}(\gamma) = \prod_{i=1}^N \mathcal{F}_{\Gamma_{VLC_i}}(\gamma) \quad (10)$$

where, $\mathcal{F}_{\Gamma_{VLC_i}}(\gamma)$ is the CDF of SNR of the i -th VLC link and is given in (6). N is the number of VLC access points. Assuming the multiple VLC links to be independent and identical, we can obtain the CDF of the best VLC link by applying Binomial approximation and making some mathematical re-arrangements in (10) as

$$\mathcal{F}_{\Gamma_{VLC}^{max}}(\gamma) = \Pr(\Gamma_{VLC}^{max} < \gamma) \simeq \vartheta^N - N\vartheta^{N-1} \chi \left(\frac{\gamma}{\bar{\gamma}_{VLC}} \right)^{\frac{-1}{m+3}} \quad (11)$$

where $\vartheta = \left(1 + \frac{L^2}{r_c^2}\right)$ and $\chi = \frac{1}{\vartheta r_c^2} (\Xi(m+1)L^{m+1})^{\frac{2}{m+3}}$

Substituting (11) and (9) in (8) we obtain the novel closed-form expression for CDF of the equivalent end-to-end SNR of the mixed FSO/VLC system as

$$\mathcal{F}_{\Gamma_{eq}}(\gamma) = K_f (1 - \vartheta^N) \gamma^{\alpha+\beta-1} \mathcal{G}_{3,7}^{6,1} \left(\left. \frac{(d\alpha\beta)^2 \gamma}{16k_2 \bar{\gamma}_{FSO}} \right|_{\tau}^{\omega} \right) + \vartheta^N - N\vartheta^{N-1} \chi \bar{\gamma}_{VLC}^{\frac{1}{m+3}} \left(\gamma \bar{\gamma}_{VLC}^{\frac{-1}{m+3}} - K_f \gamma^{\ell} \mathcal{G}_{3,7}^{6,1} \left(\left. \frac{(d\alpha\beta)^2 \gamma}{16k_2 \bar{\gamma}_{FSO}} \right|_{\tau}^{\omega} \right) \right), \quad (12)$$

where $K_f = \frac{\xi^2 2^{\alpha+\beta-2}}{\Gamma(\alpha)(2\pi)}$ and $\ell = \left(\alpha + \beta - 1 - \frac{1}{m+3}\right)$

B. Probability Density Function

Capitalizing on the derived closed-form expression of CDF, we derive the PDF of equivalent end-to-end SNR Γ_{eq} by differentiating (12) w.r.t γ . The novel closed-form expression of PDF $f_{\Gamma_{eq}}(\gamma)$ is given as

$$f_{\Gamma_{eq}}(\gamma) = K_f (1 - \vartheta^N) \gamma^{\alpha+\beta-2} \mathcal{G}_{4,8}^{6,2} \left(\left. \frac{(d\alpha\beta)^2 \gamma}{16k_2 \bar{\gamma}_{FSO}} \right|_{Y_1}^{X_1} \right) + \frac{N\vartheta^{N-1} \chi}{m+3} \bar{\gamma}_{VLC}^{\frac{1}{m+3}} (\gamma)^{-\left(\frac{m+4}{m+3}\right)} + N K_f \vartheta^{N-1} \chi \bar{\gamma}_{VLC}^{\frac{1}{m+3}} \gamma^{\ell-1} \mathcal{G}_{4,8}^{6,2} \left(\left. \frac{(d\alpha\beta)^2 \gamma}{16k_2 \bar{\gamma}_{FSO}} \right|_{Y_2}^{X_2} \right), \quad (13)$$

where $X_1 = (1 - \alpha - \beta), 1, \frac{\xi^2+1}{2}, \frac{\xi^2+2}{2}, Y_1 = \frac{\xi^2}{2}, \frac{\xi^2+1}{2}, \frac{\alpha}{2}, \frac{\alpha+1}{2}, \frac{\beta}{2}, \frac{\beta+1}{2}, 0, (2 - \alpha - \beta), X_2 = -\ell, 1, \frac{\xi^2+1}{2}, \frac{\xi^2+2}{2}$ and $Y_2 = \frac{\xi^2}{2}, \frac{\xi^2+1}{2}, \frac{\alpha}{2}, \frac{\alpha+1}{2}, \frac{\beta}{2}, \frac{\beta+1}{2}, 0, 1 - \ell$

V. PERFORMANCE EVALUATION OF MIXED FSO/VLC SYSTEM

In this section, we investigate various performance metrics for the proposed mixed FSO/VLC system and provide the closed-form expressions of outage probability and average bit error rate (BER).

A. User Outage Probability to Maintain Quality of Service (QoS)

The outage occurs when the instantaneous SNR of the link falls below the threshold SNR (γ_{th}). Thus, the outage probability can be defined by $P_{outage} = Pr[\gamma < \gamma_{th}]$. Considering the case, where the end user has a targeted threshold data rate requirement, under such condition outage probability is an important metric. The outage probability for the proposed mixed FSO/VLC system is derived by substituting $\gamma = \gamma_{th}$ in (12).

B. Average Bit Error Rate

In this section closed form expressions for average BER are derived for both the cases i.e. with and without erroneous relaying.

1) *For Perfect Relaying*: The generalized expression of average BER for a list of binary digital carrier modulation can be expressed as in [8] as

$$\mathcal{P}_e = \frac{q^p}{2\Gamma(p)} \int_0^{\infty} \gamma^{p-1} \exp(-q\gamma) \mathcal{F}_{\Gamma_{eq}}(\gamma) d\gamma, \quad (14)$$

where the constants p and q denote different modulation schemes as given in [8]. Substituting $\mathcal{F}_{\Gamma_{eq}}(\gamma)$ from (12) in (14) and using the identity [12, Eq. (2.24.3.1)] to solve the integral, we get the closed-form expressions of average BER for mixed FSO/VLC system as shown in (15), where $X_4 = (2 - \alpha - \beta - p), 1, \frac{\xi^2+1}{2}, \frac{\xi^2+2}{2}, \varsigma_1 = p+k+\alpha+\beta-1, \varsigma_2 = p+k+\alpha+\beta-1 - \frac{1}{m+3}, \Lambda(\lambda, \varsigma) = \lambda^{\varsigma} \mathcal{G}_{4,8}^{6,2} \left(\left. \frac{(d\alpha\beta)^2 \lambda}{16k_2 q \bar{\gamma}_{FSO}} \right|_{Y_5}^{X_5} \right)$ where $X_5 = 1, 1 - \varsigma, \frac{\xi^2+1}{2}, \frac{\xi^2+2}{2}, Y_5 = \frac{\xi^2}{2}, \frac{\xi^2+1}{2}, \frac{\alpha}{2}, \frac{\alpha+1}{2}, \frac{\beta}{2}, \frac{\beta+1}{2}, -\varsigma, 0$ and $\varpi(\varepsilon) = \frac{\lambda_{max} - \lambda_{min}}{\varepsilon}$

2) *For erroneous decoding*: The generalised expression of average BER for binary modulations considering decoding errors at relay node can be expressed as

$$\mathcal{P}_{e_{err}} = \mathcal{P}_{e_{FSO}} (1 - \mathcal{P}_{e_{VLC}}) + \mathcal{P}_{e_{VLC}} (1 - \mathcal{P}_{e_{FSO}}), \quad (16)$$

where $\mathcal{P}_{e_{FSO}}$ and $\mathcal{P}_{e_{VLC}}$ denotes average BER of FSO and VLC link respectively. Using equation (14) for calculating BER of individual link and then substituting them in (16) we get closed form expression as shown in (17).

VI. NUMERICAL RESULTS AND CONCLUSION

In this section, numerical results for outage probability and average BER for mixed FSO/VLC system are presented. The VLC parameters are set as $\phi_{1/2} = 60^\circ$ and optical transmitted power = 7.2 W. In Fig. 2, we observe the outage probability of the considered mixed FSO/VLC system for different FOVs of the photo-detector and for different height of LED luminaries. The FSO link is considered to have moderate atmospheric turbulence ($\alpha = 4.0, \beta = 1.9$) and number of LED luminaries used are $N = 16$. It is observed that as the FOV of the photo-detector decreases, the outage performance improves, which is quite intuitive as the FOV increases, the power of the concentrator of the photo-detector will reduce. Also it is observed as the height of LED lamps is increased the outage performance deteriorates. The Fig. 3 illustrates the functional curve for average BER vs $\bar{\gamma}_{VLC}$ keeping $\bar{\gamma}_{FSO}$ fixed at 50 dB.

$$\mathcal{P}_e = \frac{q^p}{2\Gamma(p)} \left[K_f q^{(1-\alpha-\beta-p)} \mathcal{G}_{4,7}^{6,2} \left(\frac{(d\alpha\beta)^2}{16k_2 q \bar{\gamma}_{FSO}} \Big|_{\tau}^{X_4} \right) + \sum_{j=0}^{\infty} \frac{(-q)^j}{j!} \vartheta^{N-1} \left[\vartheta \varpi(p+j) - N \chi \bar{\gamma}_{VLC}^{\frac{1}{m+3}} \varpi(p+j-1/(m+3)) \right. \right. \\ \left. \left. - \vartheta K_f (\Lambda(\lambda_{max}, \varsigma_1) - \Lambda(\lambda_{min}, \varsigma_1)) + N K_f \chi \bar{\gamma}_{VLC}^{\frac{1}{m+3}} (\Lambda(\lambda_{max}, \varsigma_2) - \Lambda(\lambda_{min}, \varsigma_2)) \right] \right] \quad (15)$$

$$\mathcal{P}_{e_{err}} = \frac{q^p}{2\Gamma(p)} \left[K_f q^{(1-\alpha-\beta-p)} \mathcal{G}_{4,7}^{6,2} \left(\frac{(d\alpha\beta)^2}{16k_2 q \bar{\gamma}_{FSO}} \Big|_{\tau}^{X_4} \right) + \sum_{j=0}^{\infty} \frac{(-q)^j}{j!} \vartheta^{N-1} \left[\vartheta \varpi(p+j) - N \chi \bar{\gamma}_{VLC}^{\frac{1}{m+3}} \varpi(p+j-1/(m+3)) \right. \right. \\ \left. \left. + K_f q^{(1-\alpha-\beta-p)} \mathcal{G}_{4,7}^{6,2} \left(\frac{(d\alpha\beta)^2}{16k_2 q \bar{\gamma}_{\tau}} \Big|_{\tau}^{X_4} \right) \left[\vartheta \varpi(p+j) - N \chi \bar{\gamma}_{VLC}^{\frac{1}{m+3}} \varpi(p+j-1/(m+3)) \right] \right] \right] \quad (17)$$

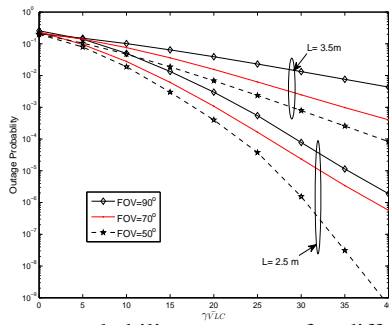


Figure 2: Outage probability vs. $\bar{\gamma}_{VLC}$ for different FOVs and room scenarios.

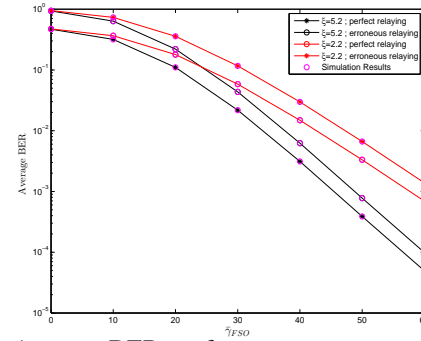


Figure 4: Average BER performance vs. $\bar{\gamma}_{FSO}$ for varying pointing error and BPSK modulation .

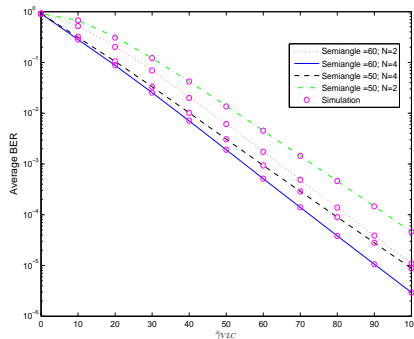


Figure 3: Average BER performance for varying number of LED luminaries and different semi angles.

The system is analysed for varying number of LEDs and for different semiangle LEDs. It can be clearly observed that the average BER decreases as the number of LEDs installed on ceiling increases. The same happen when the semiangle of the LED is increased. This is intuitive as increase in both results in an increase in coverage probability. In Fig. 4, the average BER performance versus $\bar{\gamma}_{FSO}$ keeping $\bar{\gamma}_{VLC}$ fixed at 50 dB is presented for varying pointing error. It is seen that as the pointing error decreases the BER also decreases. The average BER for erroneous decoding is also incorporated in the figure. From the results it can be seen that due to erroneous decoding at DF relay the average BER of overall system increases.

Conclusion: The performance of proposed cascaded FSO-VLC system is analysed for various indoor and outdoor parameters. The mathematical results are verified by the simulation results. The system seems to be highly feasible and efficient and thus provides an appealing solution to the spectral congestion by current broadcasting systems.

REFERENCES

- [1] A. Douik, H. Dahrouj, T. Y. Al-Naffouri and M. S. Alouini, "Hybrid Radio/Free-Space Optical Design for Next Generation Backhaul Systems," in IEEE Transactions on Communications, vol. 64, no. 6, pp. 2563-2577, June 2016.
- [2] T. Komine and M. Nakagawa, "Integrated system of white LED visible-light communication and power-line communication," in IEEE Transactions on Consumer Electronics, , vol.49, no.1, pp.71-79, Feb. 2003.
- [3] X. Ma, J. Gao, F. Yang, W. Ding, H. Yang and J. Song, "Integrated power line and visible light communication system compatible with multi-service transmission," in IET Communications, vol. 11, no. 1, pp. 104-111, 1 5 2017.
- [4] Z. Huang et al., "Hybrid Optical Wireless Network for Future SAGO-Integrated Communication Based on FSO/VLC Heterogeneous Interconnection," in IEEE Photonics Journal, vol. 9, no. 2, pp. 1-10, April 2017.
- [5] T. Komine and M. Nakagawa, "Fundamental analysis for visible-light communication system using LED lights," in IEEE Transactions on Consumer Electronics, vol. 50, no. 1, pp. 100-107, Feb 2004.
- [6] D. A. Basnayaka; H. Haas, "Design and Analysis of a Hybrid Radio Frequency and Visible Light Communication System," in IEEE Transactions on Communications , vol.PP, no.99, pp.1-1 doi: 10.1109/TCOMM.2017.2702177.
- [7] E. Zedini, I. S. Ansari and M. S. Alouini, "Performance Analysis of Mixed Nakagami-m and Gamma-Gamma Dual-Hop FSO Transmission Systems," in IEEE Photonics Journal, vol. 7, no. 1, pp. 1-20, Feb. 2015.
- [8] N. Sharma, A. Bansal and P. Garg, "Decode-and-forward relaying in mixed η - μ and gamma-gamma dual hop transmission system," in IET Communications, vol. 10, no. 14, pp. 1769-1776, 9 20 2016.
- [9] L. Yin, W. O. Popoola, X. Wu and H. Haas, "Performance Evaluation of Non-Orthogonal Multiple Access in Visible Light Communication," in IEEE Transactions on Communications, vol. 64, no. 12, pp. 5162-5175, Dec. 2016.
- [10] A. Papoulis and S.U. Pillai, "Probability, Random Variables, and Stochastic Processes," Tata McGraw-Hill Education, 2002.
- [11] P. Puri, P. Garg and M. Aggarwal, "Outage and Error Rate Analysis of Network-Coded Coherent TWR-FSO Systems," in IEEE Photonics Technology Letters, vol.26, no.18, pp.1797-1800, Sept.15, 15 2014.
- [12] A. P. Prudnikov, Y. A. Brychkov, and O. I. Marichev, *Integrals and Series: More Special Functions*, (Gordon and Breach Science Publishers, 1990, vol. 3).